

Published in final edited form as:

Curr Biol. 2005 April 12; 15(7): 603–615. doi:10.1016/j.cub.2005.02.059.

NMDA Receptors Mediate Olfactory Learning and Memory in *Drosophila*

Shouzen Xia^{1,6}, Tomoyuki Miyashita^{2,6}, Tsai-Feng Fu^{3,6}, Wei-Yong Lin³, Chia-Lin Wu³, Lori Pyzocha¹, Inn-Ray Lin³, Minoru Saitoe^{2,4}, Tim Tully¹, and Ann-Shyn Chiang^{3,5,*}

¹ Cold Spring Harbor Laboratory, 1 Bungtown Road, Cold Spring Harbor, New York 11724

² Tokyo Metropolitan Institute for Neuroscience, 2-6 Musashidai, Fuchu, Tokyo 183-8526, Japan

³ Institute of Biotechnology and Department of Life Science, National Tsing Hua University, Hsinchu 30043, Taiwan

⁴ Precursory Research for Embryonic Science and Technology, Japan Science and Technology Agency, Saitama 332-0012, Japan

⁵ Brain Research Center, National Tsing Hua University, University System of Taiwan, Hsinchu 30043, Taiwan

Summary

Background—Molecular and electrophysiological properties of NMDARs suggest that they may be the Hebbian “coincidence detectors” hypothesized to underlie associative learning. Because of the nonspecificity of drugs that modulate NMDAR function or the relatively chronic genetic manipulations of various NMDAR subunits from mammalian studies, conclusive evidence for such an acute role for NMDARs in adult behavioral plasticity, however, is lacking. Moreover, a role for NMDARs in memory consolidation remains controversial.

Results—The *Drosophila* genome encodes two NMDAR homologs, *dNR1* and *dNR2*. When coexpressed in *Xenopus* oocytes or *Drosophila* S2 cells, *dNR1* and *dNR2* form functional NMDARs with several of the distinguishing molecular properties observed for vertebrate NMDARs, including voltage/Mg²⁺-dependent activation by glutamate. Both proteins are weakly expressed throughout the entire brain but show preferential expression in several neurons surrounding the dendritic region of the mushroom bodies. Hypomorphic mutations of the essential *dNR1* gene disrupt olfactory learning, and this learning defect is rescued with wild-type transgenes. Importantly, we show that Pavlovian learning is disrupted in adults within 15 hr after transient induction of a *dNR1* antisense RNA transgene. Extended training is sufficient to overcome this initial learning defect, but long-term memory (LTM) specifically is abolished under these training conditions.

Conclusions—Our study uses a combination of molecular-genetic tools to (1) generate genomic mutations of the *dNR1* gene, (2) rescue the accompanying learning deficit with a *dNR1*⁺ transgene, and (3) rapidly and transiently knockdown *dNR1*⁺ expression in adults, thereby demonstrating an evolutionarily conserved role for the acute involvement of NMDARs in associative learning and memory.

*Correspondence: aschiang@life.nthu.edu.tw.

⁶These authors contributed equally to this work.

Accession Numbers

dNR2 sequences have been deposited in GenBank with the accession numbers AY050490 (*dNR2-1a*), AY050491 (*dNR2-1b*), AY616144 (*dNR2-1c*), AY616145 (*dNR2-1d*), AY616146 (*dNR2-1e*), AY616147 (*dNR2-1f*), AY616148 (*dNR2-2*), and AY616149 (*dNR2-3*).

Introduction

NMDA receptors (NMDARs) are one of three pharmacologically distinct subtypes of ionotropic receptors that mediate a majority of excitatory neurotransmission in the brain via the endogenous amino acid, L-glutamate. NMDARs form heteromeric complexes usually comprised of the essential NR1 subunit and various NR2 subunits [1]. The NMDAR channel is highly permeable to Ca^{2+} and Na^+ , and its opening requires simultaneous binding of glutamate and postsynaptic membrane depolarization [1–3]. Once activated, the NMDAR channel allows calcium influx into the postsynaptic cell where calcium triggers a cascade of biochemical events resulting in synaptic changes.

Cellular studies have suggested the NMDAR to be involved in several forms of synaptic plasticity, including long-term potentiation and long-term depression. The NMDAR possesses an interesting molecular property, namely a voltage-dependent blockade of glutamate-induced calcium flux, which suggests that the NMDAR may be the “Hebbian coincidence detector” underlying associative learning. Additional, non-Hebbian cellular mechanisms appear necessary, however, to model associative learning adequately [4,5]. To that end, behavioral studies attempting to demonstrate an acute role for mammalian NMDARs in associative learning and/or memory have been limited by (1) the nonspecificity of drugs that modulate NMDAR function or (2) the relatively chronic genetic manipulations of various NMDAR subunits [6–9]. Whether NMDARs also are involved with memory consolidation is even more controversial [8,10].

In invertebrates, pharmacological manipulations have suggested that NMDA-like receptors mediate associative learning in *Aplysia* [11] and memory recall in honeybee [12], and the function of an NR1 homolog, NMR-1, has been characterized in *C. elegans* [13]. These studies did not determine which potential NMDAR homologs form functional NMDARs, however [14]. More pertinently, direct demonstrations of roles for specific NMDAR genes in behavioral plasticity still are lacking in these model systems. We therefore pursued molecular, genetic, electrophysiological, and behavioral experiments on the *Drosophila* NMDAR subunit genes, *dNRI* [15] and *dNR2*, which together establish an acute role for NMDAR in associative learning and in long-term memory consolidation.

Results

The dNR Genes in *Drosophila*

We confirmed a previous report [15] by recloning the *dNRI* gene (see Supplemental Experimental Procedures available with this article online). *dNRI* is a large gene, containing 15 exons (see below). Exon 1 (noncoding) undergoes alternative splicing, giving rise to two different transcripts, which contain the same coding sequence but which differ in the 5' untranslated region. The putative *dNRI* protein from these splice forms faithfully maintains all the major structural features of NR1 receptor (Figure S3). The protein contains one hydrophobic region at the amino terminus supposedly as the signal peptide, three hydrophobic transmembrane regions (TM1, 3–4), a hydrophobic pore-forming segment in the carboxyl terminal half [14], and two ligand binding domains (S1–S2) with high homology to bacterial amino acid binding proteins [16,17]. *dNRI* also has a potential type II PDZ domain binding motif at its C terminus (X-Ψ-X-Ψ, where Ψ is a hydrophobic amino acid), suggesting interactions with other PDZ domain-containing proteins [18]. Most of the important amino acid residues for ligand binding are conserved in *dNRI*. A key asparagine residue (N631) is present in the TM2 domain and presumably controls the Ca^{2+} permeability and voltage-dependent Mg^{2+} blockade [19].

dNR2, as confirmed by complete cloning (see Supplemental Experimental Procedures), appears to be the only gene encoding the fly NR2 homolog, whereas there are four mammalian members in the NR2 subfamily [14, 20]. *dNR2* undergoes alternative splicing, mostly at the 5' untranslated region, generating eight different transcripts that may encode three different proteins (Figure 1A). Full-length cDNAs have been isolated for all eight variants. Six of them contain the same coding sequence but differ from each other at the 5' untranslated region, with five of them containing a separate noncoding exon 1. All three deduced NR2 proteins bear highest homology to NMR-2 in *C. elegans*, rat NR2D and NR2B, with respect to their overall sequence or their ligand binding and pore-forming transmembrane domains (Tables S2 and S3). Several anti-peptide monoclonal or polyclonal anti-dNR2 antibodies have been generated that specifically recognized two different bands on Westerns (Figure 1B). Because two of the putative dNR2 peptides were predicted to have similar molecular weight, it is still unclear whether the two bands in fact contained all three protein variants.

The domain structures of NR2 receptors are largely conserved in dNR2 (Figure 1C), but its general sequence homology and the active physiological sites only moderately mimic its mammalian counterparts. The protein contains four hydrophobic regions (TM1–TM4) in the carboxyl terminal half that align perfectly with the three hydrophobic transmembrane regions and a hydrophobic pore-forming segment (TM2) in other ionotropic glutamate receptors [14]. Like its rat counterpart, dNR2 has conserved major determinants of glutamate binding in the N-terminal ligand binding domain (S1) preceding transmembrane segment TM1 and the loop (S2) between TM3 and TM4 [14]. The two asparagine residues, which are present in the TM2 domain of NMDA receptors and control the Ca²⁺ permeability and voltage-dependent Mg²⁺ blockade [14], however, are not conserved in dNR2. Finally, the type I PDZ binding motif (X-S/T-X-V) is not present in dNR2, whereas it is well conserved in all vertebrate NR2 homologs [18]. Thus, *Drosophila* NMDA receptors may physically interact with PDZ domain-containing proteins through *dNR1* but not dNR2, which is usually the case in vertebrates.

Functional Expression of *Drosophila* NMDARs in *Xenopus* Oocytes or *Drosophila* S2 Cells

To determine whether these cloned *dNR1* and dNR2 subunits associate to form functional ionotropic receptor channels, we coexpressed them in *Xenopus* oocytes and examined the resulting electrophysiological properties. Coexpression of *dNR1* and dNR2-2 induced robust NMDA-selective responses (see below), whereas dNR2-1 in combination with *dNR1* induced no NMDA-dependent responses in oocytes (data not shown), suggestive of some functional difference between the two dNR2 isoforms. We have not tested coexpression of *dNR1* and dNR2-3 yet. The oocytes, expressing both *dNR1* and dNR2-2, exhibited significant inward currents upon application of NMDA but not AMPA (Figure 2A, bottom), and the NMDA-activated responses were concentration dependent (Figure 2B, top). This suggests that *dNR1* and dNR2 can form a functional ion channel in oocytes, which selectively responds to NMDA [2]. Mammalian NMDA receptors are modulated by glycine [21]. This also is the case for fly NMDA receptors (Figure 2B, middle)—although application of glutamate in the presence of glycine appears much less effective than NMDA alone, which may reflect the facts that the relevant structural domains for glycine and glutamate binding are not completely conserved in *dNR1* and dNR2 (see above) or that residual glycine may alter the response in this heterologous system (also see below). Mammalian NMDA receptors are activated by L-aspartate as well as glutamate [22]. Consistent with this observation, fly NMDA receptors are activated by various concentrations of aspartate (Figure 2B, bottom). When expressed in oocytes, however, conductance through fly NMDA receptors is not voltage dependent (data not shown). Consequently, we also coexpressed *dNR1* and dNR2 in *Drosophila* S2 cells, thereby

revealing a voltage-dependent conductance that is blocked by external Mg^{2+} (Figure 2C). Thus, this electrophysiological profile of coexpressed *dNR1* and *dNR2* reveals most of the distinguishing characteristics of vertebrate NMDARs.

Significantly, neither *dNR1* nor *dNR2* alone are sufficient to form functional receptors. Expression of *dNR1* only produced a modest response to NMDA, whereas expression of *dNR2* produced no response at all (Figure 2A, top). Thus, functional receptors require coexpression of both isoforms. This is in agreement with findings from vertebrate studies where NR1 must partner with one or more NR2 subunits to form functional NMDA channels [14].

Expression of *dNR1* and *dNR2* in Adult Brain

To examine expression of the *dNR1* protein, we generated a rabbit anti-*dNR1* polyclonal antibody. The anti-body recognized a single protein of the appropriate size on Western blot (see below). *dNR1* seems to be weakly expressed throughout the entire brain (Figures 3A and 3C; Figure S4). Higher expression levels were observed in some scattered cell bodies and part of their fibers, including those from several pairs of DPM (dorsal-posterior-medial) neurons surrounding the calyx, DAL (dorsal-anterior-lateral) and DPL (dorsal-posterior-lateral) neurons in the lateral protocerebrum (LP), VAL (ventral-anterior-lateral) neurons in the anterior protocerebrum, and two pairs of VP (ventral-posterior) neurons in the posterior protocerebrum (see also Figures 3F and 3G). Many cell bodies in the optic lobes (Figure 3A) also were labeled preferentially. Notably, punctuate staining was detected in many brain regions including the superior medial protocerebrum (Figure 3A, inset; Figure S5), suggesting synaptic localization of *dNR1*.

The anti-*dNR1* antibody does not preferentially label MB neurons. This is notable because MBs are critically required for olfactory learning [23,24]. Instead, preferential *dNR1* expression was detected in 12 pairs of cell bodies surrounding the MB calyx (Figures 3A, 3F, and 3G). Interestingly, a pair of DPM2 (dorsal-paired-medial 2) neurons are located just next to the previously identified DPM neurons in which no *dNR1* expression is detectable. The DPM neurons innervate all the MB lobes and appear involved in early memory [25]. Three additional pairs of DPM3 neurons with cell bodies smaller than DPM2 also showed strong immunolabeling. The spatial distributions of these neurons are highly symmetrical (Figures 3F and 3G). Four other DPM4 neurons are located medially to the MB calyx and send descending fibers along a common tract. DPM4 neurons are clustered together in some flies but scattered in others. Another two pairs of neurons, DPM5 and DPL (dorsal-posterior-lateral), are located above the MB calyx. They appear to project descending fibers together with DPM4 neurons (data not shown). The cell bodies of the VP (ventral-posterior) neurons are located beneath the MB calyx. DAL (dorsal-anterior-lateral) neurons are located in the LP region. LP receives extensive olfactory projections through the antennalglomerular tract of the antennal lobe, which itself receives olfactory input from antennae. The function of LP in olfaction and olfactory learning is largely unknown. *dNR1* appears only weakly expressed in antennal lobes and central complex.

One of our mouse monoclonal anti-*dNR2* antibodies allowed us to evaluate the distribution of *dNR2* proteins in adult brain. This antibody labels two bands with molecular weights close to the deduced sizes of *dNR2* proteins (Figure 1B). Similarly to *dNR1*, weak expression of *dNR2* was detected in most, if not all, brain neurons (Figures 3B and 3D). Again, preferential expression was found in several pairs of large neurons. Notably, *dNR1* and *dNR2* colocalized in four cell bodies of DPM4 neurons (Figures 3C–3E). Both proteins also colocalized in many synapse-like punctuate structures including those along the fibers of DPM4 neurons. Nevertheless, not all *dNR1*-positive neurons appear to express *dNR2* at equivalent levels or vice versa. *dNR2* is strongly expressed in a pair of DAL2 neurons and

two pairs of VAL2 neurons, for instance, whereas dNR1 is strongly expressed in DAL and VAL neurons. These observations suggest that NR1 and NR2 may be regulated differentially during development or by experience or that these subunits may partner in vivo with other unknown subunits to form functional NMDARs.

The 3D staining patterns of dNR1 and dNR2 were superimposed into a volume model of adult fly brain to analyze NR-positive fibers in more detail (Figures 3F and 3G). VAL appears to be the only neurons sending dNR1-positive projections to the front of contralateral MB calyx. Remarkably, all other NR-positive neurons do not appear to send projections to MBs. DPL and DPM5 are descending neurons and project in parallel with DPM4 neurons to the ventral-posterior ipsilateral protocerebrum and then extend anteriorly. The NR-positive fibers from other neurons surrounding the MB calyx do not enter the calyx or lobes of MBs. This, however, does not exclude the possibility that they may contact MBs through presynaptic fibers where no dNR proteins are expressed. DAL projects ascending fibers toward the superior medial protocerebrum with dNR1 protein distributed at the cell bodies and synapse-like puncta along its fibers (Figure S5). Thus, at least in DAL neurons, dNR1 appears to localize both pre- and post-synaptically.

Mutations of *dNR1* Disrupt Learning

The *dNR1* gene consists of 15 exons scanning more than 24 kb of genomic DNA [26]. The 5' end overlaps with *Itp-r83A*, the fly homolog of an inositol 1,4,5-tris-phosphate receptor. Flies homozygous for an F-element insertion in the third intron of *dNR1* are subviable and female-sterile (J. Wismar, B. Lenz-Bohme, S. Fuchs, H. Betz, and B. Schmitt, personal communication). Two independent EP element insertions also lie in *dNR1* or nearby. EP3511 inserts in the first intron of the *dNR1* gene, 718 bp upstream of the start codon in exon 2 (Figure 4A). EP331 is inserted 425 bp downstream of the 3' end of the *dNR1* transcription unit. Expression levels of dNR1 protein are reduced but not eliminated in homozygous EP3511/EP3511 or EP331/EP331 flies (Figure 4B), indicating that both EP insertions represent hypomorphic mutations of *dNR1*. EP3511/EP3511 or EP331/EP331 homozygotes are viable, which allowed us to evaluate olfactory learning [27]. Compared to wild-type flies, learning was reduced in both homozygotes (Figures 4C and 4D).

The learning defects of EP3511 or EP331 mutants were rescued by cosmids containing genomic DNA from the *dNR1* region. Cosmid-A contains the full-length *Itp-r83A* coding sequence and upstream elements that include only partial coding sequence of *dNR1*. Conversely, Cosmid-B and Cosmid-C contain all of the *dNR1* transcription unit and only part of *Itp-r83A* [28]. Cosmid-A, but not Cosmid-B or Cosmid-C, rescues the lethality associated with two different mutations of *Itp-r83A* [28], whereas Cosmid-B and Cosmid-C, but not Cosmid-A, rescued the learning defect of the EP3511 and EP331 mutants (Figures 1C and 1D). These results establish that the learning defects of the EP mutants are due to disruption of the *dNR1* gene not the *Itp-r83A* gene.

Acute Disruption of *dNR1* via an Anti-*dNR1* mRNA Produces a Learning Defect

EP331 also allowed us to use the EP-element [29] to control the expression of *dNR1* conditionally. The EP element in EP331 flies is inserted downstream of, and in an opposite orientation to, the transcription start site of *dNR1*. When combined with a GAL4 driver, this EP element yields an antisense transcript of *dNR1*. In transheterozygous EP331/+, hs-GAL4/+ flies, an anti-*dNR1* message was induced by heat shock and was still detected 15 hr later (Figure 5A), leading to a significant reduction in dNR1 protein (Figure 5B). This antisense message was also detected before heat shock in EP331/+, hs-GAL4/+ flies but absent in heterozygous EP331/+ flies (Figure 5A), suggesting some leaky expression of hs-GAL4

was driving low-level expression of anti-*dNR1*. This leaky expression did not produce any measurable effect on NR1 protein levels from Western blot analysis (Figure 5B).

The disruption of *dNR1* in EP331/+, *hs-GAL4/+* flies was further confirmed with immunohistochemistry. Anti-*dNR1* immunostaining was diminished throughout the entire brain after heat shock as compared with no heat shock (data not shown, also see Figure S4). This reduction in *dNR1* was quantified in a pair of dorsal-anterior-lateral (*DAL*) and a pair of ventral-anterior-lateral (*VAL*) neurons (Figure 5C), where the protein is expressed at high levels (Figure 3). In both *DAL* and *VAL* neurons, the immunofluorescence intensity was reduced significantly 15 hr after heat shock (Figure 5C).

Accordingly, learning was severely disrupted 15 hr after heat shock. In contrast, learning was disrupted only mildly in EP331/+, *hs-GAL4/+* flies (Figure 6A) in the absence of heat shock. This mild disruptive effect is consistent with our observation that *hs-GAL4* yields some leaky expression of anti-*dNR1* message through development (Figure 5A), though a concomitant reduction in NR1 protein was not detected. Alternatively, this transgenic line might harbor slight, nonspecific differences in genetic background.

The inducible disruption of learning also was reversible. When EP331/+, *hs-GAL4/+* flies were tested 36 hr after heat shock, learning again was largely normal (Figure 6B). Because sensorimotor responses to the odors and footshock stimuli were not affected in transheterozygous EP331/+, *hs-GAL4/+* flies before or after heat shock (Table S4), these data establish that *dNR1* is required acutely for olfactory learning.

Acute Disruption of *dNR1* Abolishes Long-Term Memory

We also evaluated whether *dNR1* was required for long-lasting memory produced by extended training [30]. EP331/+, *hs-GAL4/+* flies were subjected to spaced or massed training (see Supplemental Experimental Procedures) 15 hr after heat shock and then tested for 1-day memory (Figure 7A). In the absence of heat shock, 1-day memory after both spaced and massed training was normal. When trained 15 hr after heat shock, 1-day memory after massed training was normal, whereas that after spaced training was significantly reduced. Typically, 1-day memory after spaced training is composed of 50% LTM and 50% ARM (Anesthesia-Resistant Memory), and LTM specifically is disrupted in transgenic flies inducibly overexpressing CREB repressor. 1-day memory after massed training, in contrast, is composed only of ARM [30]. Accordingly, these results suggest that ARM is normal and LTM is completely abolished in EP331/+, *hs-GAL4/+* flies after acute disruption of *dNR1*. The observation that 1-day memory after massed training was normal also suggested that extended training might overcome the learning defect (after one training session) observed for EP331/+, *hs-GAL4/+* flies subjected to heat shock (Figure 6A). Indeed, this was the case for both spaced and massed training (Figure 7B).

For the previous experiments, we used a modified massed training protocol (cf., [30]), where flies sat in the training chamber for 150 min before training began. With this protocol, massed training ends at the same time as spaced training, but 1-day memory after massed training is slightly higher than that after our standard protocol [30], which does not include pretraining exposure to the training chamber. Hence, we repeated the above experiments with our original massed training protocol with only heat-shocked wild-type and EP331/+, *hs-GAL4/+* flies. Here again, 1-day memory after massed training was normal, whereas that after spaced training was disrupted (massed, 27 ± 4 versus 25 ± 4 ; spaced, 42 ± 4 versus 16 ± 7 ; $n = 8$ for all groups).

Disruption of *dNR1* Does Not Affect Sensorimotor Responses to Odors or Shock

Although *dNR1* was expressed throughout the adult brain and especially also at the lateral protocerebrum (LP), sensorimotor responses to the odors and foot-shock stimuli were not affected in transheterozygous EP331/+, *hs-GAL4/+* flies before or after heat shock (Table S4). Homozygous EP3511/EP3511 and EP331/EP331 mutants also performed normally to these sensory stimuli.

Discussion

Functional NMDAR in *Drosophila*

Homology searches of the *Drosophila* genome data-base and cloning suggest *dNR1* is the only gene bearing high amino acid sequence similarity to the mammalian NMDA receptor subunit NR1. Compared with its vertebrate counterpart, *dNR1* shows high homology with respect to its entire size, domain structures, and active physiological sites (Figure S3). *dNR2* appears to be the sole gene encoding the *Drosophila* homolog of mammalian NR2, although there are four NR2 family members in vertebrates [20]. *dNR2* undergoes alternative splicing, however, to generate eight different transcripts and three protein variants. The domain structures of *dNR2* show high homology to vertebrate NR2, but its entire size, active physiological sites, and molecular function are only moderately conserved from its mammalian counterparts (Figure 1C).

The *dNR1* transcript is highly regulated during development and is expressed at high levels in late embryos when the larval nervous system is formed, in late pupae when the adult central nervous system develops, and in adult head [15]. Western blots confirmed that both proteins are expressed at a high level in adult head but not in the body (data not shown). Immunostaining also indicates that they may be expressed throughout the whole brain and at especially high levels in several neurons surrounding the calyx of the MBs. The interpretation of generally weak expression of *dNR1* and *dNR2* is further supported by Western blots showing a detectable band from single-head preparations (data not shown). Thus, *dNR1* and *dNR2* likely function together in most places, which is in agreement with our functional analyses (see below). On the other hand, *dNR1* appears to have a broader pattern of preferential expression than *dNR2* in adult brain, suggesting alternative associations with other endogenous glutamate receptors. Alternatively, *dNR1* alone may form functional NMDAR channels *in vivo*, given its weak but significant NMDA-selective response in *Xenopus* oocytes (Figure 2A). It might be noted, however, that functional NMDA receptors can be formed by expression of NR1 alone in *Xenopus* oocytes but not in mammalian cell lines [14]. Finally, *dNR1* has an RSS (Retention Signal Sequence) motif at its C terminus, similar to its mammalian homolog, suggesting that *dNR1*, when not associated with *dNR2* or other glutamate receptors, may be retained in the ER rather than inserted in the cell membrane [31,32].

Coexpression of *dNR1* and *dNR2-2* in *Xenopus* oocytes generated NMDA-selective responses (Figure 2). Similarly, functional homomeric receptors can be formed within the AMPA and kainate subunit families but probably not for NMDA receptors in vertebrates, and highly active NMDAR channels are only formed when the NR1 subunit is expressed in combination with one of the four NR2 subunits [14,33]. Pharmacological, anatomical, biochemical, and immunological studies also have established heteromeric, but not homomeric, assembly of NMDAR channel subunits *in vivo* [33]. The physiological features which distinguish NMDAR from other ionotropic glutamate receptors are (1) high permeability to Ca^{2+} , (2) selective activation by NMDA and L-aspartate, (3) modulation by glycine as the coagonist for glutamate, and (4) voltage-dependent blockade by Mg^{2+} [14]. The electrophysiological profile of *dNR1* and *dNR2* coexpressed in *Xenopus* oocytes or

Drosophila S2 cells reveals that the functional NMDARs produce most of these distinguishing characteristics including selective activation by NMDA and L-aspartate, modulation by glycine as the coagonist for glutamate, and voltage- and Mg^{2+} -dependent conductance (Figure 2). Thus, *Drosophila* likely has functional NMDARs consisting of two subunits, *dNR1* and *dNR2*.

The NMDA-selective conductance was sensitive to Mg^{2+} blockade only in *Drosophila* S2 cells (Figure 2C) but not in *Xenopus* oocytes up to 10 mM (data not shown), which is highly reminiscent of NMDA receptors in *C. elegans* [13]. Proper external ionic conditions for oocytes and insect cells are remarkably different. The endogenous Mg^{2+} concentration for fly muscle, for instance, is about ten times higher than that for oocytes [34], suggesting that invertebrate NMDA receptors have evolved to be less sensitive to Mg^{2+} . Molecular evidence exists in support of this conclusion. Replacement of the asparagine residue in the pore-forming TM2 domain reduces but does not abolish Mg^{2+} block for mammalian NR receptors [14]. This crucial asparagine residue in *dNR2* subunits is replaced by glutamine. In addition, TM1, TM4, and the short linker between TM2 and TM3 domains also are critical determinants for Mg^{2+} block [35]. Although the linker appears conserved in *dNR2*, TM1 and TM4 are not (Figure 1C).

Recently, fly NMDA receptors have been shown to regulate the larval locomotor rhythm [36]. This effect can be blocked completely by MK801, requiring binding to the same asparagine residue to execute its antagonist effect [37]. MK801 also suppresses NMDAR-mediated juvenile hormone biosynthesis in cockroach [38].

NMDAR-Dependent Learning and LTM Formation in *Drosophila*

We provide the first demonstration that NMDARs are required acutely for associative learning in *Drosophila*. Our Pavlovian task is a form of fear conditioning, which uses well-defined odors as conditioned stimuli (CSs) and footshock as an unconditioned stimulus (US [27]). When tested immediately after Pavlovian conditioning (one training session), flies homozygous for either of two different hypomorphic mutations performed poorly in this task (Figure 4), although they seem to grow normally, do not show any obvious behavioral abnormalities, and most importantly, show normal sensorimotor responses to the stimuli used for this task (Table S4). The learning deficit in *dNR1* mutants can be rescued fully in transgenic flies carrying either of two different genomic constructs containing the *dNR* transcription unit, which constitutes definitive proof that this transcription unit is responsible for the phenotypic defect observed in these mutants.

dNR1 is acutely required for associative learning. Disruption of *dNR1* (Figure 5), with an *hs-GAL4* driver to induce expression of a *dNR1* antisense message, yielded a learning deficit specifically and transiently (Figure 6 and Table S4). These results rule out any potential developmental explanation for the adult learning defect. Our data extend to insects similar findings from pharmacological and genetic studies in mammals [6,7,9,39] and provide the strongest argument to date that adult learning and memory depend on proper NMDA receptor function.

Acute disruption of *dNR1* also disrupts 1-day memory after spaced training, without affecting 1-day memory after massed training (Figure 7A). The specific abolition of LTM, without affecting 1-day memory after massed training, is similar to that produced by induced expression of a CREB-repressor transgene and indicates a specific disruption of cycloheximide-sensitive LTM with no effect on cycloheximide-insensitive ARM [30]. Hence, CREB-dependent LTM formation appears to depend on normal NMDA receptor function. The cAMP/PKA/CREB signaling pathway has been shown to be involved in diverse processes ranging from hippocampal LTP and barrel formation to learning and

memory in mammals, *Drosophila* and *Aplysia* [40–51] (see also [52, 53]). In most of these experimental contexts, activation of NMDARs is required for LTM formation [7]. Recent experiments in mammals also have revealed NMDAR-dependent activation of CREB during LTP and LTM in both amygdala and hippocampus [54, 55]. Interestingly, two functionally distinct NMDA receptor signaling complexes have been identified: synaptic and extrasynaptic [56]. Synaptic NMDARs can cause sustained CREB phosphorylation and CRE-mediated gene expression, whereas extrasynaptic NMDARs actively suppress CREB activity via an as yet unknown mechanism. Hence, it seems likely that synaptic NMDAR complexes regulate memory formation by controlling nuclear signaling to CREB.

NMDAR and Behavioral Biology

Our characterization of a role for NMDA receptors in behavioral plasticity of *Drosophila* again reinforces the notion that the functional homologies among various model systems is appreciable. Many intracellular signaling proteins are known to be physically associated with vertebrate NMDA receptors [57]. The newly identified NMDAR complex consist of more than 80 different proteins, organized into receptor, adaptor, signaling, cytoskeletal, cell adhesion, and novel proteins [57]. Genetic and pharmacological disruptions of several components of the NMDAR complex produce learning impairments in rodents. Obvious *Drosophila* homologs can be identified for a majority of these 80 proteins. Among of them are NR1, PKA subunits, PKC isoforms, and NF1. Here too, disruptions of these genes yield associative learning deficits in flies (this study and [42,58,59]).

The conservation of NMDA-dependent behavioral plasticity in invertebrates further demonstrates that a unified mechanism underlies associative learning and memory. Because behavioral plasticity is tightly associated with synaptic plasticity, we speculate that similar cellular mechanisms of NMDAR-mediated long-term changes, such as LTP and LTD, may also exist in the adult insect brain. *Drosophila* genetics now can be applied to discover additional genes and signaling pathways important for NMDAR-dependent plasticity.

Conclusions

Our study establishes that *Drosophila* likely has functional NMDARs consisting of two subunits, *dNR1* and *dNR2*. Combined expression of both *dNR1* and *dNR2* generated NMDA-selective responses, whereas expression of either of them individually no significant NMDA-dependent responses in oocytes. The electrophysiological profile of *dNR1* and *dNR2* coexpressed in *Xenopus* oocytes or *Drosophila* S2 cells reveals that the functional NMDARs produce most of these distinguishing properties specific to mammalian counterparts including selective activation by NMDA and L-aspartate, modulation by glycine as the coagonist for glutamate, and voltage- and Mg^{2+} -dependent conductance.

Our study also demonstrates that NMDARs not only are involved acutely for associative learning but also are required for LTM consolidation. Genomic mutations of the essential *dNR1* gene yield defects in a Pavlovian olfactory learning task, and these learning defects are fully rescued by two different genomic transgenes containing the *dNR1*⁺ coding sequence. Importantly, we show that Pavlovian learning is disrupted within 15 hr via transient induction in adults of a *dNR1* antisense RNA transgene. Finally, the transient knockdown of *dNR1* also specifically abolishes the consolidation of protein synthesis- and CREB-dependent LTM.

Supplementary Material

Refer to Web version on PubMed Central for supplementary material.

Acknowledgments

We thank Developmental Studies Hybridoma Bank, Exelixis, Inc., Dr. P. Rorth and Dr. Y. Zhong for reagents and fly stocks, Drs. J. Wismar and B. Schmitt for fly stocks and sharing unpublished data, and Drs. H. Cline, J. Dubnau, C.-T. Ting, and S.-R. Yeh for comments and discussion. The work was supported by the National Institutes of Health and Dart Neurosciences, Inc. (T.T.), by the Naito Foundation, Kato Memorial Bioscience Foundation, and grant-in-aid from the Ministry of Education, Sciences, and Sports Culture of Japan (M.S.), and by the National Science Council, the Brain Research Center of the University System of Taiwan, and the Technology Development Program of Ministry of Economy, National Center for High-performance Computing, and Dart Neurosciences, Inc. (A.S.C.). T.T. is a paid consultant to Helicon Therapeutics, Inc. As a cofounder of Helicon, he owns less than 5% of the company.

References

1. McBain CJ, Mayer ML. N-methyl-D-aspartic acid receptor structure and function. *Physiol Rev* 1994;74:723–760. [PubMed: 8036251]
2. Monaghan DT, Bridges RJ, Cotman CW. The excitatory amino acid receptors: their classes, pharmacology, and distinct properties in the function of the central nervous system. *Annu Rev Pharmacol Toxicol* 1989;29:365–402. [PubMed: 2543272]
3. Nowak L, Bregestovski P, Ascher P, Herbet A, Prochiantz A. Magnesium gates glutamate-activated channels in mouse central neurones. *Nature* 1984;307:462–465. [PubMed: 6320006]
4. Abbott LF, Nelson SB. Synaptic plasticity: taming the beast. *Nat Neurosci* 2000;307(Suppl):1178–1183. [PubMed: 11127835]
5. Debanne D, Daoudal G, Sourdet V, Russier M. Brain plasticity and ion channels. *J Physiol (Paris)* 2003;97:403–414. [PubMed: 15242652]
6. Morris RG, Anderson E, Lynch GS, Baudry M. Selective impairment of learning and blockade of long-term potentiation by an N-methyl-D-aspartate receptor antagonist, AP5. *Nature* 1986;319:774–776. [PubMed: 2869411]
7. Riedel G, Platt B, Micheau J. Glutamate receptor function in learning and memory. *Behav Brain Res* 2003;140:1–47. [PubMed: 12644276]
8. Shimizu E, Tang YP, Rampon C, Tsien JZ. NMDA receptor-dependent synaptic reinforcement as a crucial process for memory consolidation. *Science* 2000;290:1170–1174. [PubMed: 11073458]
9. Tsien JZ, Huerta PT, Tonegawa S. The essential role of hippocampal CA1 NMDA receptor-dependent synaptic plasticity in spatial memory. *Cell* 1996;87:1327–1338. [PubMed: 8980238]
10. Day M, Morris RG. Memory consolidation and NMDA receptors: discrepancy between genetic and pharmacological approaches. *Science* 2001;293:755. [PubMed: 11486056]
11. Roberts AC, Glanzman DL. Learning in *Aplysia*: looking at synaptic plasticity from both sides. *Trends Neurosci* 2003;26:662–670. [PubMed: 14624850]
12. Si A, Helliwell P, Maleszka R. Effects of NMDA receptor antagonists on olfactory learning and memory in the honeybee (*Apis mellifera*). *Pharmacol Biochem Behav* 2004;77:191–197. [PubMed: 14751445]
13. Brockie PJ, Mellem JE, Hills T, Madsen DM, Maricq AV. The *C. elegans* glutamate receptor subunit NMR-1 is required for slow NMDA-activated currents that regulate reversal frequency during locomotion. *Neuron* 2001;31:617–630. [PubMed: 11545720]
14. Dingledine R, Borges K, Bowie D, Traynelis SF. The glutamate receptor ion channels. *Pharmacol Rev* 1999;51:7–61. [PubMed: 10049997]
15. Ultsch A, Schuster CM, Laube B, Betz H, Schmitt B. Glutamate receptors of *Drosophila melanogaster*. Primary structure of a putative NMDA receptor protein expressed in the head of the adult fly. *FEBS Lett* 1993;324:171–177. [PubMed: 8508917]
16. Kuryatov A, Laube B, Betz H, Kuhse J. Mutational analysis of the glycine-binding site of the NMDA receptor: structural similarity with bacterial amino acid-binding proteins. *Neuron* 1994;12:1291–1300. [PubMed: 8011339]
17. Stern-Bach Y, Bettler B, Hartley M, Sheppard PO, O'Hara PJ, Heinemann SF. Agonist selectivity of glutamate receptors is specified by two domains structurally related to bacterial amino acid-binding proteins. *Neuron* 1994;13:1345–1357. [PubMed: 7527641]

18. Sheng M, Sala C. PDZ domains and the organization of supramolecular complexes. *Annu Rev Neurosci* 2001;24:1–29. [PubMed: 11283303]
19. Burnashev N, Schoepfer R, Monyer H, Ruppersberg JP, Gunther W, Seeburg PH, Sakmann B. Control by asparagine residues of calcium permeability and magnesium blockade in the NMDA receptor. *Science* 1992;257:1415–1419. [PubMed: 1382314]
20. Yamakura T, Shimoji K. Subunit- and site-specific pharmacology of the NMDA receptor channel. *Prog Neurobiol* 1999;59:279–298. [PubMed: 10465381]
21. Kleckner NW, Dingledine R. Requirement for glycine in activation of NMDA-receptors expressed in *Xenopus* oocytes. *Science* 1988;241:835–837. [PubMed: 2841759]
22. Patneau DK, Mayer ML. Structure-activity relationships for amino acid transmitter candidates acting at N-methyl-D-aspartate and quisqualate receptors. *J Neurosci* 1990;10:2385–2399. [PubMed: 2165523]
23. de Belle JS, Heisenberg M. Associative odor learning in *Drosophila* abolished by chemical ablation of mushroom bodies. *Science* 1994;263:692–695. [PubMed: 8303280]
24. Connolly JB, Roberts IJ, Armstrong JD, Kaiser K, Forte M, Tully T, O’Kane CJ. Associative learning disrupted by impaired Gs signaling in *Drosophila* mushroom bodies. *Science* 1996;274:2104–2107. [PubMed: 8953046]
25. Waddell S, Armstrong JD, Kitamoto T, Kaiser K, Quinn WG. The amnesiac gene product is expressed in two neurons in the *Drosophila* brain that are critical for memory. *Cell* 2000;103:805–813. [PubMed: 11114336]
26. Adams MD, Celniker SE, Holt RA, Evans CA, Gocayne JD, Amanatides PG, Scherer SE, Li PW, Hoskins RA, Galle RF, et al. The genome sequence of *Drosophila melanogaster*. *Science* 2000;287:2185–2195. [PubMed: 10731132]
27. Tully T, Quinn WG. Classical conditioning and retention in normal and mutant *Drosophila melanogaster*. *J Comp Physiol [A]* 1985;157:263–277.
28. Acharya JK, Jalink K, Hardy RW, Hartenstein V, Zuker CS. InsP3 receptor is essential for growth and differentiation but not for vision in *Drosophila*. *Neuron* 1997;18:881–887. [PubMed: 9208856]
29. Rorth P. A modular misexpression screen in *Drosophila* detecting tissue-specific phenotypes. *Proc Natl Acad Sci USA* 1996;93:12418–12422. [PubMed: 8901596]
30. Tully T, Preat T, Boynton SC, Del Vecchio M. Genetic dissection of consolidated memory in *Drosophila*. *Cell* 1994;79:35–47. [PubMed: 7923375]
31. Scott DB, Blanpied TA, Swanson GT, Zhang C, Ehlers MD. An NMDA receptor ER retention signal regulated by phosphorylation and alternative splicing. *J Neurosci* 2001;21:3063–3072. [PubMed: 11312291]
32. Standley S, Roche KW, McCallum J, Sans N, Wenthold RJ. PDZ domain suppression of an ER retention signal in NMDA receptor NR1 splice variants. *Neuron* 2000;28:887–898. [PubMed: 11163274]
33. Mori H, Mishina M. Structure and function of the NMDA receptor channel. *Neuropharmacology* 1995;34:1219–1237. [PubMed: 8570021]
34. Stewart BA, Atwood HL, Renger JJ, Wang J, Wu CF. Improved stability of *Drosophila* larval neuromuscular preparations in haemolymph-like physiological solutions. *J Comp Physiol [A]* 1994;175:179–191.
35. Kuner T, Schoepfer R. Multiple structural elements determine subunit specificity of Mg²⁺ block in NMDA receptor channels. *J Neurosci* 1996;16:3549–3558. [PubMed: 8642401]
36. Cattaert D, Birman S. Blockade of the central generator of locomotor rhythm by noncompetitive NMDA receptor antagonists in *Drosophila* larvae. *J Neurobiol* 2001;48:58–73. [PubMed: 11391649]
37. Ferrer-Montiel AV, Sun W, Montal M. Molecular design of the N-methyl-D-aspartate receptor binding site for phencyclidine and dizolcipine. *Proc Natl Acad Sci USA* 1995;92:8021–8025. [PubMed: 7644531]
38. Chiang AS, Lin WY, Liu HP, Pszczolkowski MA, Fu TF, Chiu SL, Holbrook GL. Insect NMDA receptors mediate juvenile hormone biosynthesis. *Proc Natl Acad Sci USA* 2002;99:37–42. [PubMed: 11773617]

39. Blair HT, Schafe GE, Bauer EP, Rodrigues SM, LeDoux JE. Synaptic plasticity in the lateral amygdala: a cellular hypothesis of fear conditioning. *Learn Mem* 2001;8:229–242. [PubMed: 11584069]
40. Silva AJ, Kogan JH, Frankland PW, Kida S. CREB and memory. *Annu Rev Neurosci* 1998;21:127–148. [PubMed: 9530494]
41. Brandon EP, Idzerda RL, McKnight GS. PKA isoforms, neural pathways, and behaviour: making the connection. *Curr Opin Neurobiol* 1997;7:397–403. [PubMed: 9232801]
42. Dubnau J, Tully T. Gene discovery in *Drosophila*: new insights for learning and memory. *Annu Rev Neurosci* 1998;21:407–444. [PubMed: 9530502]
43. Abdel-Majid RM, Leong WL, Schalkwyk LC, Smallman DS, Wong ST, Storm DR, Fine A, Dobson MJ, Guernsey DL, Neumann PE. Loss of adenylyl cyclase I activity disrupts patterning of mouse somatosensory cortex. *Nat Genet* 1998;19:289–291. [PubMed: 9662407]
44. Mayford M, Kandel ER. Genetic approaches to memory storage. *Trends Genet* 1999;15:463–470. [PubMed: 10529810]
45. Frankland PW, Josselyn SA, Anagnostaras SG, Kogan JH, Takahashi E, Silva AJ. Consolidation of CS and US representations in associative fear conditioning. *Hippocampus* 2004;14:557–569. [PubMed: 15301434]
46. Pittenger C, Huang YY, Paletzki RF, Bourtchouladze R, Scanlin H, Vronskaya S, Kandel ER. Reversible inhibition of CREB/ATF transcription factors in region CA1 of the dorsal hippocampus disrupts hippocampus-dependent spatial memory. *Neuron* 2002;34:447–462. [PubMed: 11988175]
47. Falls WA, Kogan JH, Silva AJ, Willott JF, Carlson S, Turner JG. Fear-potentiated startle, but not pre-pulse inhibition of startle, is impaired in CREB α Delta α mutant mice. *Behav Neurosci* 2000;114:998–1004. [PubMed: 11085615]
48. Kida S, Josselyn SA, de Ortiz SP, Kogan JH, Chevere I, Masushige S, Silva AJ. CREB required for the stability of new and reactivated fear memories. *Nat Neurosci* 2002;5:348–355. [PubMed: 11889468]
49. Cho YH, Giese KP, Tanila H, Silva AJ, Eichenbaum H. Abnormal hippocampal spatial representations in alphaCaMKII α 286A and CREB α Delta α mice. *Science* 1998;279:867–869. [PubMed: 9452387]
50. Kogan JH, Frankland PW, Blendy JA, Coblenz J, Marowitz Z, Schutz G, Silva AJ. Spaced training induces normal long-term memory in CREB mutant mice. *Curr Biol* 1997;7:1–11. [PubMed: 8999994]
51. Bourtchouladze R, Frenguelli B, Blendy J, Cioffi D, Schutz G, Silva AJ. Deficient long-term memory in mice with a targeted mutation of the cAMP-responsive element-binding protein. *Cell* 1994;79:59–68. [PubMed: 7923378]
52. Gass P, Wolfer DP, Balschun D, Rudolph D, Frey U, Lipp HP, Schutz G. Deficits in memory tasks of mice with CREB mutations depend on gene dosage. *Learn Mem* 1998;5:274–288. [PubMed: 10454354]
53. Rammes G, Steckler T, Kresse A, Schutz G, Zieglansberger W, Lutz B. Synaptic plasticity in the basolateral amygdala in transgenic mice expressing dominant-negative cAMP response element-binding protein (CREB) in forebrain. *Eur J Neurosci* 2000;12:2534–2546. [PubMed: 10947828]
54. Schulz S, Siemer H, Krug M, Holtt V. Direct evidence for biphasic cAMP responsive element-binding protein phosphorylation during long-term potentiation in the rat dentate gyrus in vivo. *J Neurosci* 1999;19:5683–5692. [PubMed: 10377374]
55. Cammarota M, Bevilaqua LR, Ardenghi P, Paratcha G, Levi de Stein M, Izquierdo I, Medina JH. Learning-associated activation of nuclear MAPK, CREB and Elk-1, along with Fos production, in the rat hippocampus after a one-trial avoidance learning: abolition by NMDA receptor blockade. *Brain Res Mol Brain Res* 2000;76:36–46. [PubMed: 10719213]
56. Hardingham GE, Fukunaga Y, Bading H. Extra-synaptic NMDARs oppose synaptic NMDARs by triggering CREB shut-off and cell death pathways. *Nat Neurosci* 2002;5:405–414. [PubMed: 11953750]
57. Husi H, Ward MA, Choudhary JS, Blackstock WP, Grant SG. Proteomic analysis of NMDA receptor-adhesion protein signaling complexes. *Nat Neurosci* 2000;3:661–669. [PubMed: 10862698]

58. Guo HF, Tong J, Hannan F, Luo L, Zhong Y. A neurofibromatosis-1-regulated pathway is required for learning in *Drosophila*. *Nature* 2000;403:895–898. [PubMed: 10706287]
59. Drier EA, Tello MK, Cowan M, Wu P, Blace N, Sacktor TC, Yin JC. Memory enhancement and formation by atypical PKM activity in *Drosophila melanogaster*. *Nat Neurosci* 2002;5:316–324. [PubMed: 11914720]
60. Wollmuth LP, Kuner T, Sakmann B. Adjacent asparagines in the NR2-subunit of the NMDA receptor channel control the voltage-dependent block by extracellular Mg²⁺. *J Physiol* 1998;506:13–32. [PubMed: 9481670]

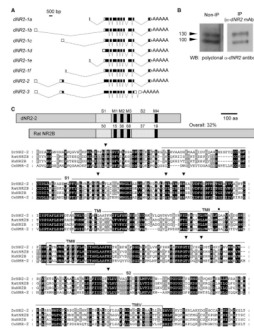


Figure 1. Cloning and Molecular Characterization of *dNR2*

(A) *dNR2* variants, generated via alternative splicing, are shown. Six variants (*dNR2-1a–dNR2-1f*) encode the same protein but differ from each other at the 5' untranslated region. *dNR2-2* differs from *dNR2-1* at the 5' end, where it contains an extra coding exon 2. *dNR2-3* differs from *DrNR2-1* at the 5' end, containing the same extra coding exon 2 and two different exons at the 3' end.

(B) Anti-*dNR2* antibodies recognize at least two proteins on immunoblots. Protein extracts from wild-type fly heads were blotted directly (left) or first were immunoprecipitated with a monoclonal anti-*dNR2* antibody (right) and then probed with a polyclonal anti-*dNR2* antibody. Both antibodies specifically recognize at least two *dNR2* proteins.

(C) Predicted domain structure and amino acid sequence of *dNR2*. (Top) Protein domains in *dNR2* and rat NR2B receptor, with the percent amino acid identity between the homologs indicated. Abbreviations are as follows: M1–4, transmembrane domain 1–4; S1–S2, ligand binding domains 1 and 2. (Bottom) Putative amino acid sequence of *dNR2* and its alignment with rat and human NR2B and NMR-2 in *C. elegans*. The *dNR2* sequence is numbered beginning from the first predicted methionine. The open boxes indicate the transmembrane domains. The underlined regions indicate the two ligand binding domains (S1–S2) with high homology to bacterial amino acid binding proteins. The conserved residues for glycine binding are marked with arrow heads. The asparagine residue, for controlling the Ca^{2+} permeability and voltage-dependent Mg^{2+} blockade [19,60], is replaced with a glutamine (Q722) in *dNR2* (closed circle).

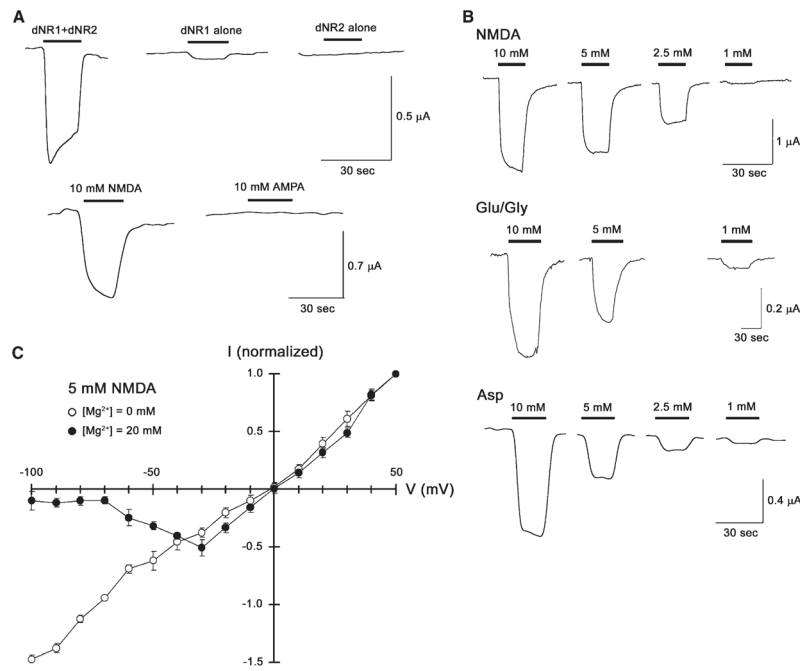


Figure 2. Coexpression of *dNR1* and *dNR2-2* Yields a Functional NMDA Receptor

(A) NMDA response in *Xenopus* oocytes expressing both *dNR1* and *dNR2-2*. Oocytes injected with *dNR1* and *dNR2-2* cRNAs exhibited inward currents upon application of NMDA (10 mM) but not upon application of AMPA (10 mM; bottom). Oocytes expressing *dNR1* alone showed modest inward currents upon application of 10 mM NMDA, whereas the oocytes expressing *dNR2-2* alone showed no significant NMDA-selective responses (top). This suggests that *dNR1* and *dNR2* subunits function as heterodimers to form the functional NMDA channels.

(B) NMDA, glutamate in combination with glycine, and L-aspartate activate fly NMDA receptors in a concentration-dependent manner. Besides NMDA (top), coexpression of *dNR1* and *dNR2-2* can be activated by glutamate in the presence of glycine as coagonist (Glu/Gly, middle) and by L-aspartate (Asp, bottom). In each case, current responses were observed in the dosage-dependent manner.

(C) Voltage dependence of NMDAR in *Drosophila* S2 cells. Coexpression of *dNR1* and *dNR2-2* yields a voltage-dependent effect on conductance (mean \pm SEM, same for all of the following figures) at a physiological concentration of Mg²⁺ (20 mM), but conductance is linear in the absence of external Mg²⁺ (n = 8).

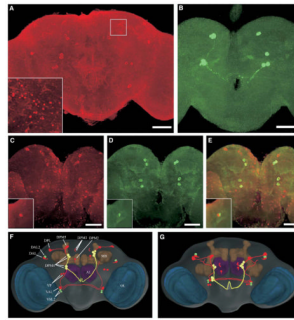


Figure 3. dNR1 and dNR2 Proteins Are Expressed in Adult Brain

(A) Confocal imaging of dNR1 immunostaining in the whole-mount adult brain (posterior view). All neurons show weak expression of *dNR1* (some nonspecific immunostaining cannot be ruled out; see text), whereas preferential expression is found in cell bodies distributed throughout the central brain and optical lobes. Inset: synapse-like immunopositive structures are detected in the superior medial protocerebrum (white square; also see Figure S5).

(B) Immunolabeling of dNR2 proteins (posterior view). Again, weak immunostaining is detected in most neurons with preferential expression in several big neurons.

(C–E) Double labeling of *dNR1* and dNR2 (posterior view); *dNR1* staining is shown in red (C) and dNR2 in green (D). (E) Shown is a merged image of *dNR1* and dNR2 antibody staining. Bar, 50 μm . Insets: dorsal-anterior-lateral protocerebrum (anterior view).

(F and G) dNR circuits in the *Drosophila* brain model. The most prominent neuropil regions are color coded: blue, optic lobes; brown, mushroom bodies; purple, antennal lobes; rest of brain, gray. Two representative sets of original confocal series of *dNR1* and dNR2 immunolabeling images are 3D reconstructed and transformed into the brain volume model. The spatial relationship between dNR circuits and brain neuropils is analyzed with Amira volume rendering. Cell bodies and fibers showing (1) predominant and preferential *dNR1* (red) or dNR2 (green) or (2) similar but preferential expression of both (yellow) are traced with Photoshop. (F) Posterior view; (G) Dorsal posterior view. AL, antennal lobes; MB, mushroom bodies; OL, optic lobes; DAL, dorsal-anterior-lateral; DPL, dorsal-posterior-lateral; DPM, dorsal-posterior-medial; VAL, ventral-anterior-lateral; VP, ventral-posterior.

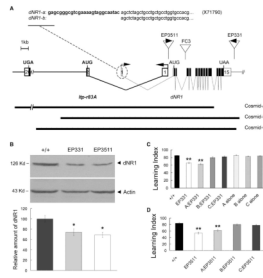


Figure 4. Hypomorphic Mutations of *dNRI* Disrupt Olfactory Learning

(A) Molecular characterization of *dNRI*. The *dNRI* transcription unit is complicated by its overlap with *Itp-r83A* (fly homolog of Inositol 1,4,5-tris-phosphate receptor). The *dNRI* gene consists of 15 exons (open boxes, noncoding exons; closed boxes, coding regions). *dNRI* generates two different transcripts via alternative splicing of noncoding exon 1. The insertion sites for EP3511, EP331, and FC3 are shown as are the genomic fragments contained in Cosmids-A, -B, and -C.

(B) *dNRI* protein from Western blot analysis is severely disrupted in EP331 and EP3511 homozygous mutants. *dNRI* levels were normalized to those of actin and were quantified from nine replicate experiments. As compared with wild-type flies (+/+), *dNRI* was reduced significantly (asterisk) in EP331 and EP3511 mutants (bottom).

(C) Olfactory “learning” (memory retention quantified 3 min after one training session) is disrupted in EP331 homozygous mutants (double asterisk, $P < 0.001$), and this learning defect is rescued in EP331 homozygous mutants, carrying Cosmid-B or Cosmid-C, but not Cosmid-A, transgenes. Wild-type flies carrying any of the three Cosmid transgenes (A, B, or C alone) showed normal learning.

(D) Olfactory learning is disrupted significantly in EP3511 homozygous mutants (double asterisk, $P < 0.001$), and again, this learning defect is rescued by Cosmid-B or Cosmid-C transgenes.

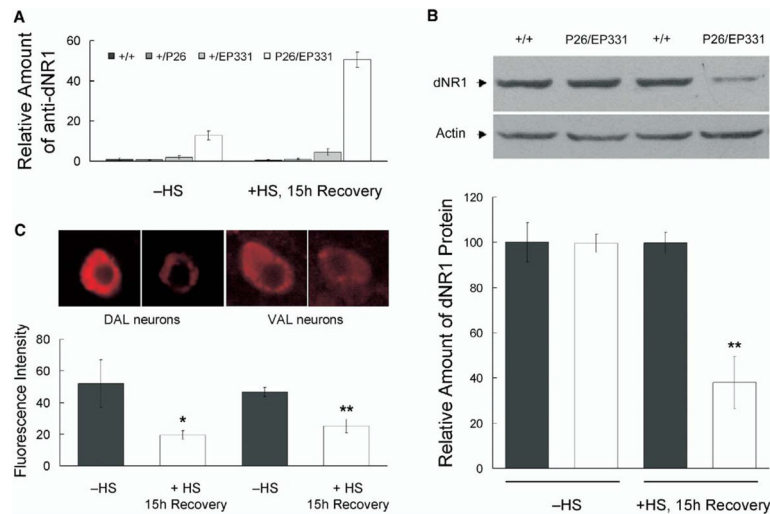


Figure 5. Acute Induction of Anti-*dNR1* mRNA Disrupts *DNR1*

(A) Q-PCR reveals the induction of an antisense RNA after heat shock in EP331/+, *hs-GAL4*/+ flies (P26/EP331). Homozygous EP331 virgins were crossed to *hs-GAL4* (P26) males. As controls, EP331 (+/EP331) or *hs-GAL4* (+/P26) flies were crossed to wild-type flies. All the crosses were maintained at 18°C to minimize the leaky expression of *hs-GAL4*. 1- to 2-day-old flies were harvested from above crosses, subjected to a 7 hr heat-shock protocol, and then allowed to recover for 15 hr at 18°C (+HS, 15 hr Recovery; see Supplemental Experimental Protocol for details). Different groups of flies were treated in parallel but were not subjected to heat shock (-HS), serving as controls for possible nonspecific effect from handling during heat shock. RNAs then were isolated from heads, and Q-PCR was used to quantify induction of the anti-*dNR1* mRNA.

(B) *dNR1* protein was disrupted upon induction of the anti-*dNR1* mRNA. Western blotting indicated that *dNR1* was diminished after heat shock in EP331/+, *hs-GAL4*/+ (P26/EP331) but not in wild-type (+/+) flies. For a loading control, the same blot was probed with anti-actin antibody. *dNR1* levels were quantified from four replicate experiments (bottom; double asterisk, $P < 0.001$).

(C) Expression of *dNR1* also is diminished in situ. Induced expression of anti-*dNR1* was quantified in a pair of dorsal-anterior-lateral (DAL) and a pair of ventral-anterior-lateral (VAL) neurons, where the protein is preferentially expressed (see Figure 3). In both cases, expression of *dNR1* was significantly reduced (bottom; asterisk, $P < 0.05$; double asterisk, $P < 0.001$).

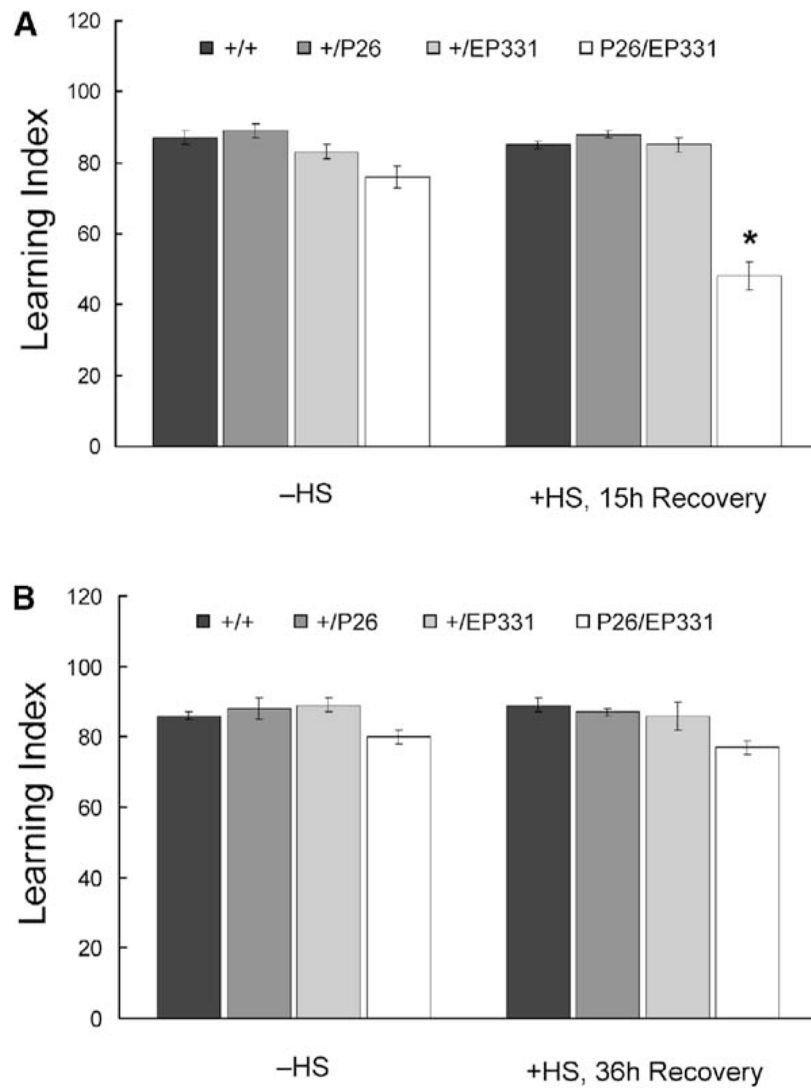


Figure 6. Olfactory Learning Is Disrupted by Acute Induction of Anti-*dNRI* mRNA

(A) Learning in transheterozygous EP331/+, *hs-GAL4*/+ (P26/EP331) flies is significantly reduced after heat shock (+HS, 15 hr Recovery; asterisk, $P < 0.001$) and is slightly lower in the absence of heat shock (-HS). Heterozygous *hs-GAL4* (+/P26) and EP331 (+/EP331) flies with or without heat shock perform similarly to wild-type controls (+/+).

(B) When tested 36 hr after heat shock, learning in EP331/+, *hs-GAL4*/+ flies is similar to those without heat shock, suggesting that the heat shock-specific disruption of learning is transient.

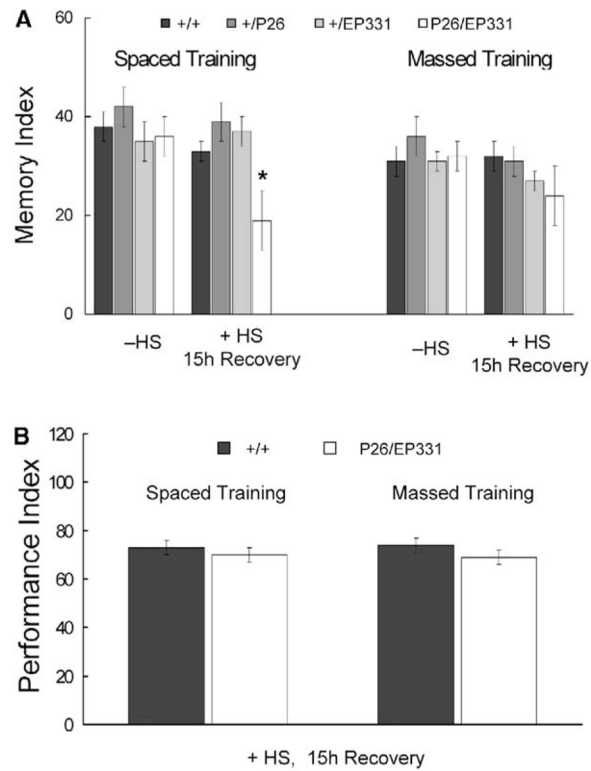


Figure 7. Acute Induction of Anti-*dNRI* mRNA Specifically Abolishes LTM

(A) EP331/+, *hs-GAL4/+* (P26/EP331) flies were subjected to spaced or massed training (see Supplemental Experimental Procedures) 12–15 hr after heat shock. 1-day memory after spaced training is significantly disrupted (asterisk, $P < 0.05$), whereas that after massed training is normal. 1-day memory after spaced training in EP331/+, *hs-GAL4/+* flies is reduced 47%.

(B) When tested immediately after spaced or massed training, learning was normal in EP331/+, *hs-GAL4/+* flies after heat shock, suggesting that repetitive training can overcome the transient learning defect observed after one training session.